

Corrosion Protection of Carbon Steel by *Pongamia glabra* Oil-Based Polyetheramide Coatings

Manawwer Alam^{1,*}, Naser M Alandis², Naushad Ahmad², Mohammad Asif Alam³

¹ Research Centre-College of Science, King Saud University, P.O. Box 2455, Riyadh 11451, Saudi Arabia

² Department of Chemistry, College of Science, King Saud University, P.O. Box 2455, Riyadh 11451, Saudi Arabia

³ Center of Excellence for Research in Engineering Materials, Advanced Manufacturing Institute (AMI), King Saud University, P. O. Box 800, Al-Riyadh 11421, Saudi Arabia

*E-mail: malamiitd@gmail.com

Received: 27 September 2017 / Accepted: 4 January 2018 / Published: 5 February 2018

Application of electrochemical techniques for corrosion studies of polyetheramide (PEtA) coatings on carbon steel is considered using electrochemical impedance spectroscopy (EIS) and potentiodynamic polarization studies, which are powerful techniques to better understand the fundamental process of corrosion. In this paper, these techniques are discussed in detail as complementary approaches to understand the complex nature of coating degradation. The PEtA coating was synthesized from a *Pongamia glabra* oil-based fatty amide diol and bisphenol A. The synthesis was confirmed by Fourier transform infrared spectroscopic techniques. The PEtA coatings were applied on carbon steel strips and their physico-mechanical properties, such as scratch hardness, impact, conical mandrel, and pencil hardness tests, were characterized by standard methods. The surface morphology of the coatings was observed by scanning electron microscopy, and their thermal stability was assessed by thermogravimetric analysis. The anticorrosion properties of PEtA were assessed in a 3.5 wt% NaCl solution at room temperature using potentiodynamic polarization and EIS techniques. The PEtA coatings exhibit good physico-mechanical and anticorrosive properties for applications up to 350 °C.

Keywords: polyetheramide; coatings; potentiodynamic; corrosion; EIS.

1. INTRODUCTION

Vegetable oils are considered to be one of the most important classes of sustainable sources of starting materials for the production of coatings [1–3]. Different types of polymers have been prepared from these oils using a variety of polymerization techniques, including those involving free radical, condensation, metathesis, and addition reactions [4]. Seed oils such as soybean, linseed, nahar (*Mesua*

ferrea), cotton, jatropha, *Pongamia glabra*, tung, castor, rapeseed (*Brassica napus*), and neem (*Azadirachta indica*) have been used to prepare different polymeric resins by appealing to the characteristic properties of the individual oils resulting from their unique fatty acid composition [5–8]. In this way, vegetable seed oils have been used to synthesize several types of polymeric resin such as alkyds, polyesteramides, polyetheramides, polyurethanes, and epoxies [9–12], which have found use in various applications like paints, coatings, adhesives, binders, and composites [13]. Polymeric coatings protect metals by forming a barrier against oxygen and H^+ ions, which reduces the rate of corrosion [14–16].

Based on alternating current and voltage, electrochemical impedance spectroscopy (EIS) has been widely used in corrosion studies because it can clarify corrosion mechanisms. EIS is a linear technique determined in the frequency domain that is capable of measuring electrochemical properties across a wide range of frequencies. Moreover, in a single experimental procedure, EIS can encompass a sufficiently broad range of frequencies to distinguish between applied potentials. For this reason, the technique is gaining popularity in diffusion studies of ions across membranes and in studies of semiconductor interfaces. Additionally, EIS has been applied to investigate the kinetics of corrosion reactions, corrosion inhibitors, anodic coatings, and polymer coatings. A central feature of EIS is impedance, which is a proportionality factor between current and voltage. In corrosion applications, EIS consists of measuring the impedance of the coated metal in solution. EIS is a non-destructive method that can determine various parameters like polymer capacitance, film resistance, and the metal–coating interface [17, 18].

Impedance can be calculated using Ohm's law as:

$$Z(\omega) = \frac{E(\omega)}{i(\omega)}$$

As a complex number, impedance $Z(\omega)$ can be represented in Cartesian as well as polar coordinates.

$$Z(\omega) = |Z(\omega)|e^{j\varphi}$$

Where $|Z(\omega)|$ is the magnitude of the impedance and φ is the phase shift.

In Cartesian coordinates, impedance given by:

$$Z(\omega) = Z'(\omega) - j.Z''(\omega)$$

Where $Z'(\omega)$ is the real component of the impedance, $Z''(\omega)$ is the imaginary component, $j = \sqrt{-1}$, and ω is angular frequency ($2\pi f$). The relationship between these two approaches for representing data can be given by:

$$|Z|^2 = |Z'|^2 + (-Z'')^2$$

$$\tan(\varphi) = \frac{-Z''}{Z'}$$

Alternatively, the real and imaginary components can be obtained from:

$$Z' = |Z|\cos\varphi$$

$$-Z'' = -|Z|\sin\varphi$$

As seen, impedance can be described by the frequency and phase angle, θ or alternatively by its real and imaginary components. The mathematical convention for separating the real and imaginary

components is to multiply the magnitude of the imaginary component by $j [= \sqrt{-1}]$ and report the real and imaginary values as a complex number [17, 19].

The response of an electrode to alternating potential signals of varying frequency is interpreted on the basis of circuit models of the electrode/electrolyte interface.

$$Z_{real} = R_s + \frac{R_c}{1 + (\omega R_c C_c)^2}$$

$$Z_{imag} = \frac{-\omega C_c (R_c)^2}{1 + (\omega R_c C_c)^2}$$

In an electrochemical process, the corrosion process assumes that electron transfer at the metal surface governs the rate of both the anodic and cathodic reactions.

In electrochemical impedance analysis, three different types of plots are commonly used: Nyquist plots (complex plane, showing $-Z_{imag}$ versus Z_{real}) and two different types of Bode plots (i.e. impedance magnitude versus log frequency and angle theta versus log frequency). Nyquist plots provide a single capacitive semicircle that indicates the occurrence of charge transfer, whereas Bode and phase angle plots indicate systems with equivalent circuits.

The open circuit potential (OCP) is the potential of the working electrode relative to a reference electrode when no potential or current is applied to the cell. When a potential is applied relative to the open circuit, the system measures the OCP before the cell is turned on and then applies the potential relative to that measurement [20]. The OCP is the potential difference between the working and reference electrodes when they are immersed in an electrolyte. Positive OCPs indicate that E_{oc} will accelerate oxidation (corrosion) reactions, whereas reduction reactions will be accelerated if the applied voltage is more negative than E_{oc} . The potentiostat controls the potential between the working and reference electrodes, while it measures the current between the working and counter electrodes. A plot of log I versus E is called a Tafel plot. Compliance voltage is the voltage available at the counter electrode that can be used to force current to flow and still maintain control of the working electrode voltage. Compliance voltage can become important when the currents are high or when the conductivity of the solution is low. In practice, this depends on the electrolyte and cell design, and is representative of a cell with an electrolyte of low conductivity. Finally, since the reference electrode is often placed relatively close to the working electrode, there is less impedance than that between the counter and working electrodes.

Organic polymeric coatings have gained increased attention as corrosion protectants of carbon steel (CS) systems because of their effectiveness in different environments. In this article, polyetheramide was synthesized from *Pongamia glabra* oil and then coated onto CS substrates. The coated panels were then studied by standard physico-mechanical and corrosion resistance investigations. Broadly, it is expected that the significance of this work will benefit both industry and the environment as *Pongamia glabra* oil-based polyetheramide coatings were found to improve the corrosion resistance of CS considerably. Without question, improved corrosion resistance of mild steel in saline environments would motivate various industries to use these materials as leverage to gain a competitive business advantage.

2. EXPERIMENTAL

2.1. Materials

Pongamia glabra oil was extracted from seeds using a Soxhlet apparatus with petroleum ether (BP 60–80 °C). The fatty acid composition of this oil was reported previously by our group [11]. Diethanolamine (Winlab, UK), bisphenol A (Merck, India), sodium chloride, methanol, xylene, butanone, and petroleum ether (BDH Chemicals, Ltd. Poole, England) were used as received without further purification.

2.2. Characterization

The FTIR spectra of N,N'-bis(2-hydroxy ethyl) *Pongamia glabra* oil fatty amide (HEPFA) and PEtA were measured using an FTIR spectrophotometer (Spectrum 100, Perkin Elmer, USA) with NaCl cells. The thermal stability of these resins was assessed by thermogravimetric analysis (TGA)/DSC1 (Mettler Toledo AG, Analytical CH-8603, Schwerzenbach, Switzerland) in a nitrogen atmosphere at a heating rate of 10 °C/min. The PEtA resin molecular weight was determined by gel permeation chromatography (GPC) (HT-GPC Module 350A, Viscotek, Houston, TX, USA) with tetrahydrofuran (THF) as the eluent at a flow rate of 1.0 mL/min. The resin morphology was examined by scanning electron microscopy (SEM) (JEOL, JED-2200 Series, Japan). Additionally, the physico-chemical characteristics such as the iodine value (ASTM D5556), hydroxyl value (ASTM D1957-86), specific gravity (ASTM D1475), and refractive index (ASTM D1218) (Abbe Refractometer, Model R-4, Rajdhani Scientific Instruments Co., India) of the resin were also determined. The physico-mechanical properties of the coating were evaluated by impact resistance (IS 101: Part 5/Sec 3, 1988), scratch hardness (BS 3900), crosshatch adhesion (ASTM D3359-02), the conical mandrel bend test (ASTM D3281-84), and the pencil hardness test (ASTM) (Wolff–Wilborn tester, Sheen Instruments, England). Finally, the coating thickness (Elcometer Coating Thickness Gauge, Model 456; Elcometer Instruments, Manchester, UK) and gloss (Glossmeter, Model: KSJ MG6-F1, KSJ Photoelectrical Instruments Co., Ltd., Quanzhou, China) were also evaluated.

Potentiodynamic polarization and EIS were measured by an Autolab potentiostat/galvanostat, PGSTAT204-FRA32, with the NOVA software (Metrohm Autolab B.V. Kanaalweg 29-G, 3526 KM, Utrecht, The Netherlands) using a three-electrode system at room temperature. The counter and references electrodes were platinum and the saturated calomel electrode, respectively. As the working electrode, the coated metal specimens were covered by a fixed PortHoles electrochemical sample mask with an exposed surface area of 1.0 cm² in 3.5% NaCl corrosive media. Potentiodynamic polarization (PDP) was performed at a sweep rate of 10 mV s⁻¹ in the potential range ±250 mV with respect to the OCP. Each coating system was evaluated in triplicate for its ability to resist corrosion. EIS spectra were obtained in the frequency range of 100 Hz to 1 MHz with an amplitude of 10 mV with 10 points per decade at the corrosion potential.

2.3. Synthesis of *N, N'*-bis(2-hydroxy ethyl) *Pongamia glabra* oil fatty amide (HEPFA)

HEPFA was synthesized as per a previously reported method [11].

2.4. Synthesis of *Pongamia* oil-based polyetheramide (PEtA)

PEtA was synthesized as per a previously reported method [6].

2.5. Coating preparation and testing

The PEtA resin was dissolved in a 40% solution of xylene and butanone (1:1). The resultant solution was applied by the dip technique to differently sized mild steel panels for the corrosion tests (30 mm × 10 mm × 1 mm) and the physico-mechanical tests (70 mm × 25 mm × 1 mm). When the coated panels became dry to touch at room temperature, they were cured by baking at 180±5 °C for 20 min, which hardened the coating. The PEtA coating thickness was determined to be 125±5 μm. The physico-mechanical tests of the PEtA coating included: gloss (65), impact resistance (150 lb/in), scratch hardness (3.0 kg), crosshatch adhesion (100%), pencil hardness test (5H), and bending test (1/8 inch conical mandrel). The PEtA coating showed good results in terms of gloss, scratch hardness, impact resistance, and bending. Overall, these results indicate good adhesion of the coating to the mild steel substrate, which was made possible by the presence of polar hydroxyl groups, amide linkages, and aromatic rings of bisphenol A molecules within the coating.

3. RESULTS AND DISCUSSION

3.1. Spectral analysis of HEPFA and PEtA

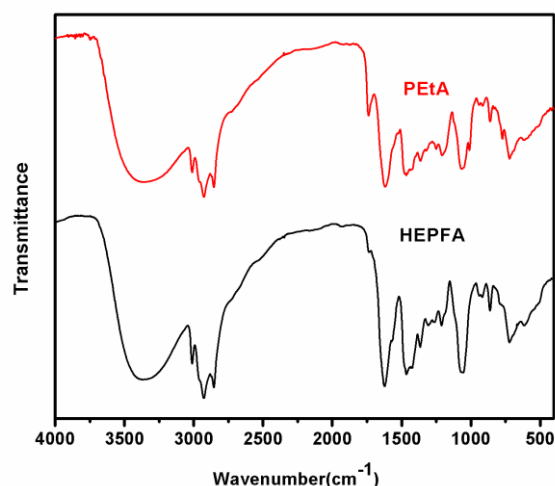


Figure 1. FTIR Spectra of *N, N'*-bis(2-hydroxy ethyl) *Pongamia glabra* oil fatty amide (HEPFA) and polyetheramide (PEtA)

As seen in Figure 1, key features of the FTIR spectrum of HEPFA include: 3363 cm^{-1} , OH stretch; 3014 cm^{-1} , -CH=CH- stretch; 2854 and 2925 cm^{-1} , CH_2 symmetrical and asymmetrical stretches, respectively; 1620 cm^{-1} , carbonyl amide stretch; and 1468 cm^{-1} , -C-N- stretch. The FTIR spectrum of PEtA shows additional bands at 1229 cm^{-1} , -C-O-C- asymmetrical stretch; 1082 cm^{-1} , -C-O-C- symmetrical stretch; and 3052 , 1588 , 1513 , and 726 cm^{-1} , aromatic ring stretches. These peaks support the formation of PEtA from HEPFA.

3.2. Physicochemical analysis

Decreases of the hydroxyl value (from 8.50 to 6.39) and the iodine value (from 57.00 to 41.23) are evident on the conversion of HEPFA to PEtA. These trends indicate the loss of hydroxyl groups of HEPFA and bisphenol A during the condensation reaction. The refractive index value of HEPFA (1.4758) increases in PEtA (1.5430), suggesting an increase in molecular weight on moving from HEPFA to PEtA. The molecular weight of PEtA was determined to be 6048 Daltons (Mw and Mn), with a polydispersity index of 1.68.

3.3. Tafel analysis

The ability of the PEtA coatings to resist corrosion on mild steel coupons was evaluated by the Tafel extrapolating method. Specifically, this approach involved determining the open circuit potential, polarization resistance, and corrosion current density (i_{corr}) after immersion for 5, 10, 15, 20, 25, and 30 days in 3.5 wt.% NaCl solutions. Figure 2 shows the Tafel plots for the bare CS and the PEtA-coated panels. As seen, the corrosion potential shifts toward more anodic potential as the immersion time increases, as also listed in Table 1. R_p is the resistance to charge transport through pores, voids, and other defects in a polymer coating [21–25].

Table 1. Corrosion parameters for bare carbon steel (CS) and PEtA coated CS after in 3.5% NaCl solution

Immersion time	$\beta_a(\text{V})$	$\beta_c(\text{V})$	$E_{\text{corr}}(\text{v})$	$I_{\text{corr}}(\text{A})$	C R (mm/year)	LPR ($\Omega \cdot \text{cm}^2$)
CS,1h	0.114	0.691	-0.596	3.526E-05	0.410	1207.3
5 days	0.365	0.354	-0.0484	1.877E-09	2.205E-05	4.116E+07
10 days	0.404	0.400	0.0658	2.148E-09	2.496E-05	4.062E+07
15 days	0.397	0.381	-0.0638	2.440E-09	2.836E-05	3.462E+07
20 days	0.364	0.329	-0.0011	3.310E-09	3.845E-05	2.271E+07
25 days	0.382	0.381	-0.0718	3.312E-09	3.848E-05	2.499E+07
30 days	0.383	0.334	-0.0648	2.916E-09	3.889E-05	2.666E+07

Bierwagen et al. reported that the polarization (R_p) value for organic coatings lies between 10^9 and $10^{10}\ \Omega \cdot \text{cm}^2$, and lies between 10^6 and $10^9\ \Omega \cdot \text{cm}^2$ for a good coating. The coating is considered poor if the R_p value is less than $10^6\ \Omega \cdot \text{cm}^2$ [16].

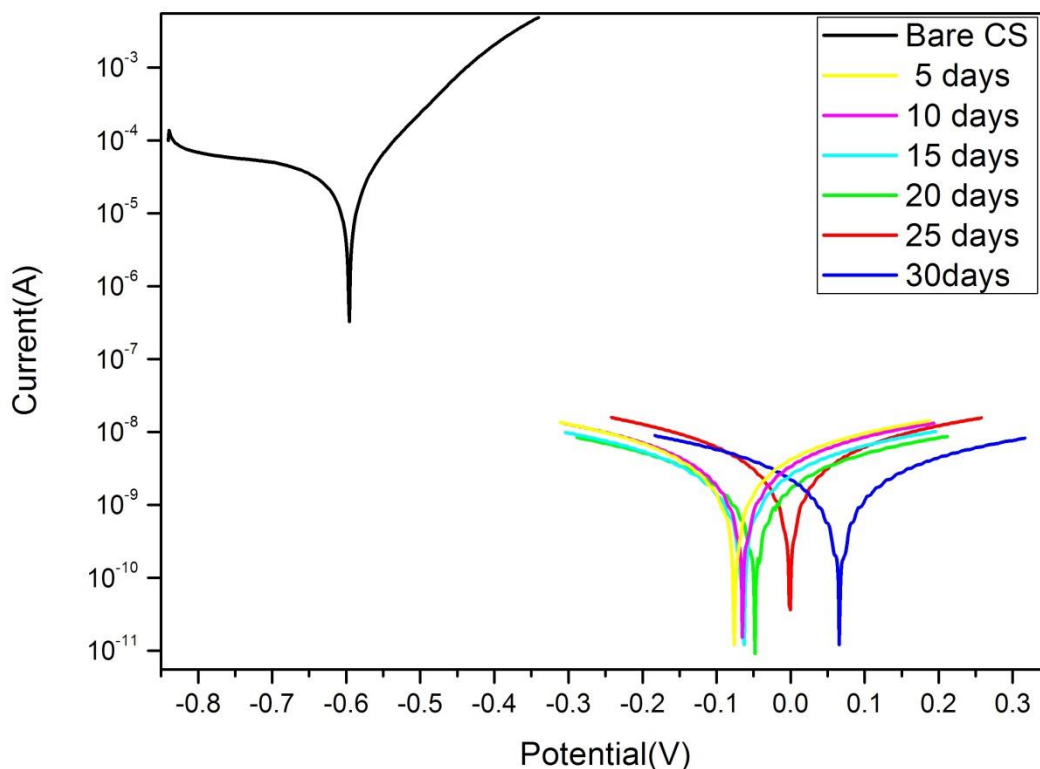


Figure 2. Tafel plots of bare CS and PEtA coated carbon steel after immersion in 3.5% NaCl solution

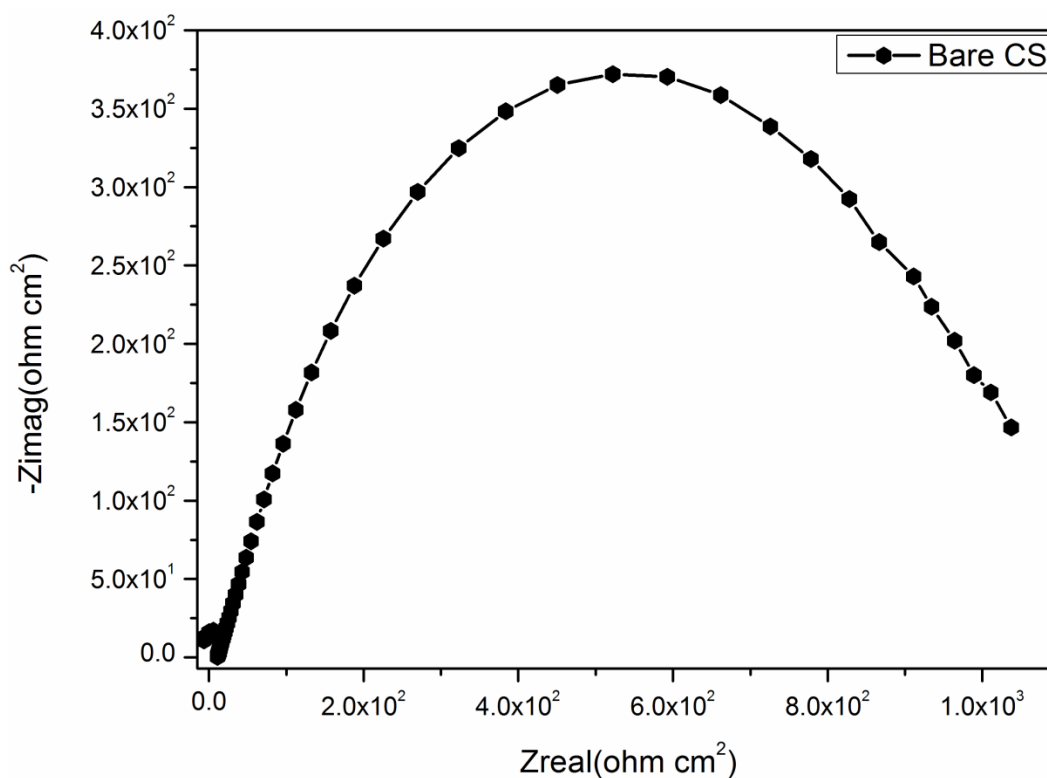
3.4. Electrochemical impedance spectroscopy (EIS)

The Nyquist plot obtained from the EIS measurements of the bare CS specimen after 1 h immersion is shown in Figure 3. Additionally, Nyquist plots for the PEtA-coated CS samples following exposure to aerated 3.5 wt.% NaCl aqueous solutions after 5, 10, 15, 20, 25, and 30 days immersion are also shown. The impedance parameters like R_s , R_{ct} , and C_c are presented in Table 2. All of the obtained Nyquist plots appear semicircle in nature, with the semicircle diameters changing as a function of the coating immersion time [26, 27]. For the semicircles at the higher and lower frequency ends, the intercepts correspond to R_s and $R_s + R_{ct}$, respectively. The difference between the two values is the charge transfer resistance, R_{ct} , which provides a measure of electron transfer across the surface and is inversely proportional to the rate of corrosion [28–30]. The presence of a semicircle indicates the formation of a barrier on the metal-coated surface for electron transfer and that charge-transfer processes primarily control the CS corrosion process. The capacitance values are only associated with the coating. These values provide a measure of water permeation into the coating due to the development of charge at the coating–electrolyte interface. R_s is the solution resistance and depends on the resistivity of the solution and the location of the reference electrode with respect to the working electrode. After 30 days of immersion, the coating begins to degrade and behave as a loss dielectric. Eventually, the coating degrades to the point at which corrosion can occur at lower frequencies, provided that the solution is conducting. The electrolyte distribution inside the film is uniform, having penetrated through the coating pores; a heterogeneous distribution parallel to the surface occurs where

it does not distribute in a uniform way. In this case, migration of ions from the solution to the metal surface via the polymer chain becomes more difficult.

Table 2. Impedance data obtained by simulation in 3.5% NaCl solution

Immersion Time (days)	Rs(Ω)	Rct(Ω)	Cc(F)	CPE(n)
Bare CS	25.363	1054.7	1.046E-03	0.996
5	-3667.2	1.342E+07	1.186E-11	0.998
10	-4607.98	1.196E+07	4.255E-11	0.998
15	-7295.1	1.380E+07	7.915E-11	0.998
20	-7866.3	1.294E+07	1.230E-10	0.997
25	-3794.4	6.353E+06	1.746E-10	0.997
30	-2765.3	8.988E+06	1.770E-10	0.998



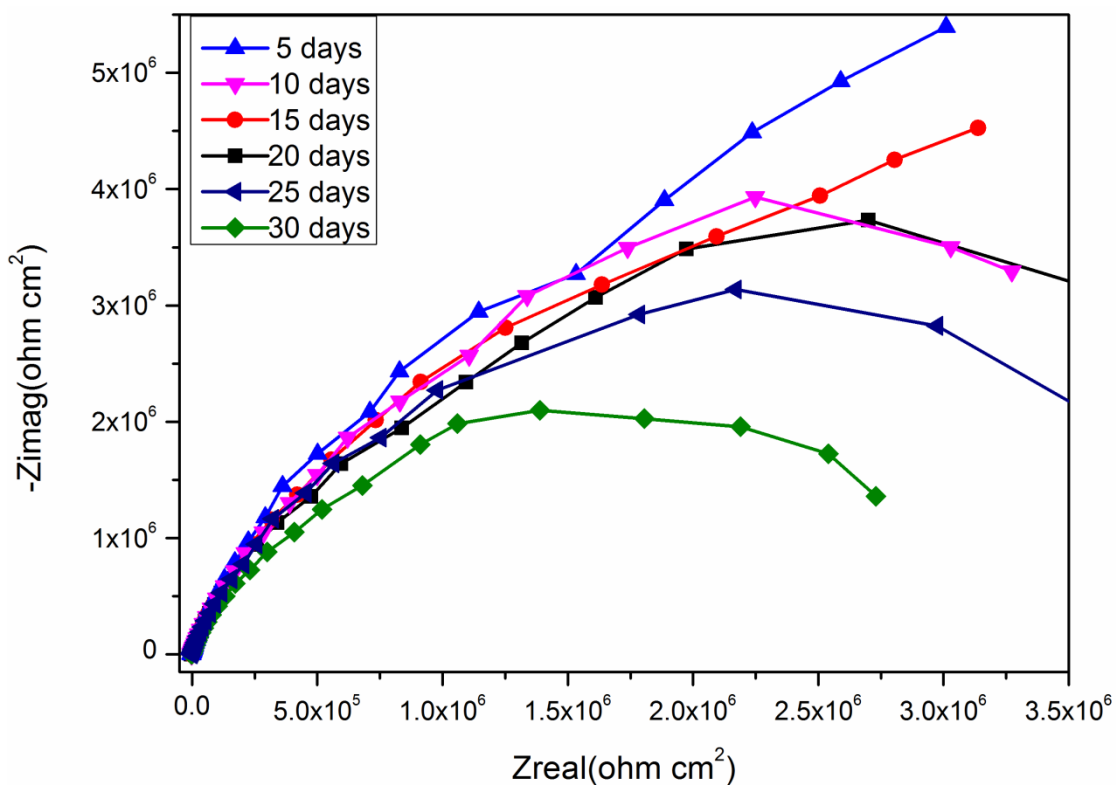


Figure 3. Nyquist plots of bare CS and PETa coated carbon steel after immersion in 3.5% NaCl solution

The properties of PETa make it useful for application in aqueous medium because it is a polar organic coating [28–35]; indeed, the presence of amide, ether, and hydroxyl groups in its structure, as well as lone pairs of electrons, causes effective binding with mild steel, which may be facilitated by vacant d orbitals of iron. A small distortion was observed in the Nyquist diagrams after prolonged immersion time; this distortion has been attributed to frequency dispersion [36–41]. It is clear from all plots that the impedance response of CS in the NaCl solution changed significantly with immersion time. The diameters of the capacitive loop decreased on increasing the immersion period, indicating the extent of the corrosion process. Single capacitive semicircles were observed for all PETa coatings until 30 days of immersion. Relative to pristine CS, the PETa-coated CS samples exhibited relatively high R_{ct} values [42,43].

Pure capacitance is indicated by fitting the obtained results to constant phase element (CPE) values nearest a value of 1 [36, 37]. These high R_{ct} values are related to low charge-transfer resistance between the CS and the PETa-coated CS samples.

3.5. Thermal analysis

Figure 4 shows TGA thermograms of HEPFA and PETa. The thermal stability of PETa increases following the incorporation of bisphenol A. An initial 5% weight loss is observed at 262 °C and 383 °C for HEPFA and PETa, respectively, which is attributed to the evaporation of trapped solvent. The 50 wt% loss at 442 °C and 510 °C for HEPFA and PETa, respectively, is attributed to the

degradation of amide linkages, while the 80 wt% loss observed at 497 °C and 534 °C for these compounds, respectively, can be attributed to the degradation of hydrocarbons (aliphatic and aromatic). The HEPFA thermogram shows two decomposition events, whereas only one sharp decomposition event occurs for PEtA. This result indicates that the HEPFA monomer has free OH, amide, and alkyl chain groups, whereas all the functional groups in the PEtA polymer are engaged in the polymer chain.

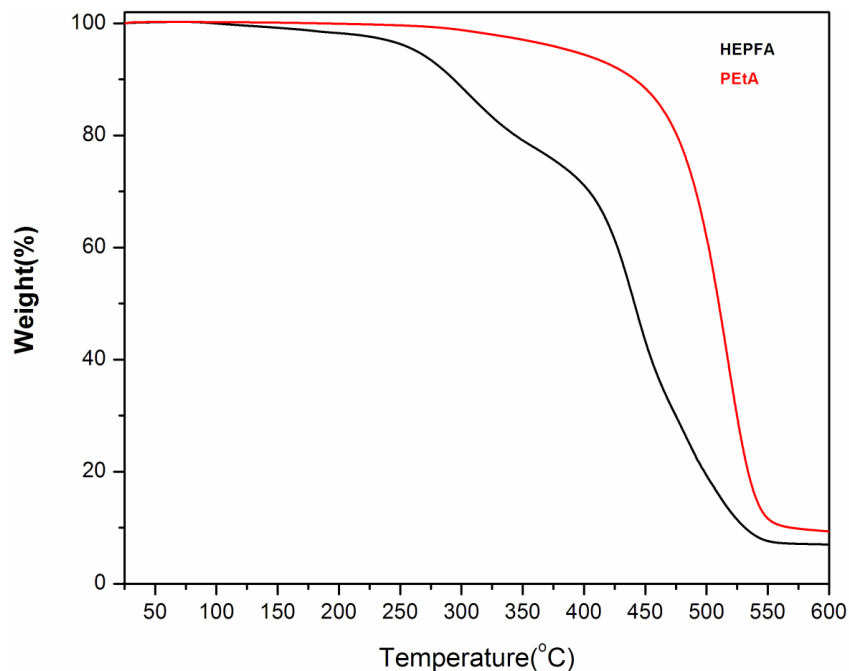


Figure 4. TGA thermogram of HEPFA and PEtA

3.6. SEM analysis

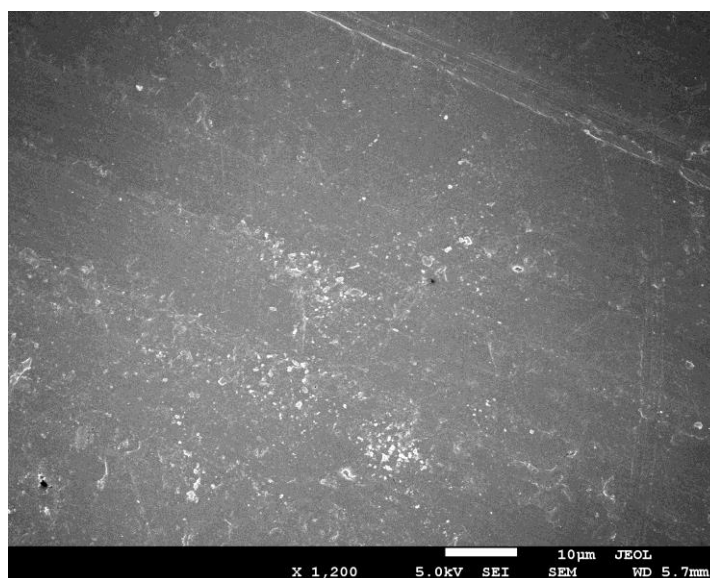


Figure 5. SEM micrograph of coated PEtA after immersion in 3.5% NaCl solution

The SEM micrograph of the PEtA coatings after immersion in the NaCl solution shows that it is unaffected in this environment (Figure 5); slight salt deposition is evident on the surface. The said medium is unable to penetrate the coating and reach the substrate; that is, the coating does not lose adhesion with the substrate and shows no dissolution or further deterioration in the NaCl solution.

4. CONCLUSIONS

Pongamia glabra oil is a promising source for polyetheramide (PEtA) coating materials. The PEtA coating is composed of ether and amide functional groups and fatty acid chains, making it an ideal candidate to protect carbon steel (CS) from corrosion because of its good adherence to the CS surface. The PEtA coating showed good scratch hardness, flexibility, gloss, and can be safely used up to 350 °C as an eco-friendly coating material. PEtA coatings on CS provide very effective protection against corrosion as a result of their good adhesion to the CS substrate and their effective barrier properties. The potentiodynamic polarization and electrochemical impedance spectroscopic results indicated that PEtA exhibited significant corrosion protection for CS against the corrosion electrolyte (NaCl) at room temperature; the PEtA coating resistance was in excess of $10^6 \Omega \text{ cm}^2$ after 30 days of immersion.

ACKNOWLEDGEMENT

The Project was supported by King Saud University, Deanship of Scientific Research, College of Science - Research Center.

References

1. Y. Xia, Z. Zhang, M. R. Kessler, B.B. Stecher and R. C. Larock, *ChemSusChem*, 5 (2012) 2221.
2. S. D. Rajput, V. V. Gite, P. P. Mahulikar, V. R. Thamke, K. M. Kodam and A. S. Kuwar, *J. Am. Oil Chem. Soc.*, 91(2014) 1055.
3. A. Chaudhari, R. Kulkarni, P. Mahulikar, D. Sohn and V. Gite, *J. Am. Oil Chem. Soc.*, 92(2015)733.
4. C. Fu, Z. Yang, Z. Zheng and L. Shen, *Prog. Org. Coat.*, 77(2014)1241.
5. H. A. El-Wahab, M. A. E. L. Fattah and M.B.M. Ghazy, *Prog. Org. Coat.*, 72 (2011) 353.
6. S. Ahmad, S.M. Ashraf, E. Sharmin, M. Nazir and M. Alam, *Prog. Org. Coat.*, 52 (2005) 85.
7. P. D. Meshram, R. G. Puri, A. L. Patil and V. V. Gite, *Prog. Org. Coat.*, 76 (2013) 1144.
8. O. Rahman, M. Kashif and S. Ahmad, *Prog. Org. Coat.*, 80(2015)77.
9. A. Chaudhari, A. Kuwar, P. Mahulikar, D. Hundiwale, R. Kulkarni and V. Gite, *RSC Adv.*, 4(2014) 17866.
10. M. Alam and N. M. Alandis, *High Perform. Polym.*, 24(6)(2012)538.
11. M. Alam and N. M. Alandis, *Pigm. Res. Technol.*, 42/3(2013)195.
12. M. A. Alam, U. A. Samad, R. Khan, M. Alam and S. M. Al-Zahrani, *Korean J. Chem. Eng.*, 38(2017) 2301.
13. M. Alam and N. M Alandis, US Patent 8,946,351 B1, Feb 3,2015.
14. M. Alam, N. M. Alandis and N. Ahmad, *Int. J. Poly. Anal. Charact.*, 22(2017)281.
15. S.B. Lyon, R. Bingham and D.J. Mills, *Prog. Org. Coat.*, 102(2017)2.

16. G.P. Bierwagen, L. He, J. Li, L. Ellingson and D.E. Tallman, *Prog. Org. Coat.*, 39(2000)67.
17. U. Rammelt and G. Reinhard, *Prog. Org. Coat.*, 21(1992)205.
18. A.S. Castela, and A.M. Simoes. *Corros., Sci.*45 (2003)1631.
19. Z.M. Elimat. *J. Compos. Mater.*, 49(1)(2015)3.
20. M. A. Ameer and A.M. Fekry, *Prog. Org. Coat.*, 71(2011)343.
21. S. Frangini. *Mater and Corros.*, 57(2006)330.
22. N.N. Voevodin, V.N. Balbyshev, M. Khobaib and M.S. Donley. *Prog. Org. Coat.*, 47(2003)416.
23. B. Lengyel, L. Meszaros, G. Meszaros, E. Fekete, F. Janaszik and I. Szenes, *Prog. Org. Coat.*, 36(1999)11.
24. E. H. Saarivirta, V. E. Yudin, L.A. Myagkova and V.M. Svetlichnye, *Prog. Org. Coat.*, 72(2011)269-278.
25. F. Li, G-xi. Li, J. Zeng and G-hong Gao, *J. Appl. Polym. Sci.*, 131(2014)40602.
26. C. Corfias, N. Pebere and C. Lacabanne, *Corros. Sci.*, 42(2000)1337.
27. J-T. Zhang, J-M. Hu, J-Q. Zhang and C-N Cao, *Prog. Org. Coat.*, 51(2004)145.
28. Yan-Hua Liu, Xiao-Han Jin and Ji-Ming Hu, *Corros. Sci.*, 106(2016)127.
29. W. Li, H. Tian and B. Hou. *Mater. and Corros.* 61(2010)1.
30. Y. Gonzalez-Garcia, S. Gonzalez and R.M. Souto, *Corros. Sci.*, 49(2007)3514.
31. M. Behzadsab, S.M. Mirabedini, K. Kabiri and S. Jamil, *Corros. Sci.*, 53(2011)89.
32. L. Fedrizzi, F. Andreatta, L. Paussa, F. Deflorian and S. Maschio, *Prog. Org. Coat.*, 63(2008)299.
33. A. S. Shin and M. Y. Shon, *J. Ind. Eng. Chem.*, 16(2010)884.
34. M. Heidarian, M.R. Shishesaz, S.M. Kassiriha and M. Nematollahi, *Prog. Org. Coat.*, 68(2010) 180.
35. M.C.S.S. Macedo, I.C.P. Margrit-Mattos, F.L. Fragata, J.B. Jorcin, N. Pebere and O.R. Mattos, *Corros. Sci.*, 51(2009)1322.
36. B. Ramezanzadeh, A. Ahmadi and M. Mahdavian, *Corros. Sci.*, 109(2016)182.
37. S. Pourhashem, M. R.Vaezi, A.Rashidi and M. R.Bagherzadeh. *Corros. Sci.*, 115(2017)78.
38. X. Li, Z.Weng, W. Yuan, X. Luo, H. M. Wong, X. Liu, S.Wu, K.W.K. Yeung, Y. Zheng and P. K. Chu. *Corros. Sci.*, 102(2016)209.
39. M.G. Hosseini, M. Sabouri and T. Shahrabi, *Prog. Org. Coat.*, 60(2007)178.
40. G.
41. Grundmeir, W. Schmidt and M. Stratmann, *Electrochimica Acta.*, 45(2000)2515.
42. S.F.L. Mertens and E. Temmerman, *Corros. Sci.*,43(2001)69.
43. M. A. Albuquerque, M. C. C. de Oliveira and A. Echevarria, *Int. J. Electrochem. Sci.*, 12 (2017) 852.
44. M. A. Alam, U. A. Samad, E-S. M. Sherif, O. Alothman, A. H. Seikh and S. M. Al-Zahrani *Int. J. Electrochem. Sci.*, 12 (2017) 74.